Electrode Design for Wire Interconnected Back Contact Solar Cells

A. Spribille, J. D. Huyeng, T. Schweigstill, I. Franzetti, L. C. Rendler and F. Clement
Fraunhofer Institute for Solar Energy Systems ISE,
Heidenhofstraße 2, 79110 Freiburg, Germany
Phone: +49 (0)761 4588 5538
e-mail: alma.spribille@ise.fraunhofer.de

ABSTRACT: Back contact back junction (BC-BJ) solar cells are a well-studied cell concept for high efficiency silicon solar cells. Wire interconnection is a known approach for the interconnection of solar cells with electrodes on front and rear side but has only recently been investigated in combination with back contact concepts [1]. Here, an optimal electrode design has quite different requirements. This study determines the smallest possible electrode geometry for linear electrodes on BC-BJ solar cells by conducting peel tests on geometry variations. Moreover, it is shown that the reliability of the wire interconnection is improved by implementing an optimized H-shaped pad geometry. Consequently, the H-shape is applied on BC-BJ half-cells and evaluated based on peel force measurements, as well as electroluminescence images of wire interconnected half-cells. A significant increase of peel force from below 0.1 N for linear pads to above 0.3 N for H-shaped pads, as well as a significant decrease of failure rate from 12.5 % for linear pads down to 4.5 % are demonstrated

Keywords: back contact, wire interconnection, bifacial

1 INTRODUCTION AND MOTIVATION

Back contact solar cells concepts have mainly been investigated on cell level or in combination with module interconnection based on ribbons and conductive backsheets. The minimized front side shading due to wire interconnection does not apply to back contact concepts as they have all metal contacts on the rear side. Probably due to that reason, wire interconnection has not yet been published in detail for back contact concepts.

Besides the reduced shading, wire interconnection features some advantages which do apply to back contact concepts like reduced mechanical stress and therefore less bowing. Furthermore, the electrode design can be designed irrespective of optical aspects targeting other parameters in a BC-BJ optimized design. While the mechanical stress has been investigated by Rendler *et al.* [1], no investigation on the optimized electrode designs have been carried out so far.

Optimized electrode geometries can increase the solar cell efficiency of BC-BJ cells by reducing recombination on the metal-semiconductor interface (j_{0met}) without additional process steps like insulation layers and local contact opening (LCO). Optimized doping structures enabled by optimized electrode geometries allow minimal electrical shading. At the same time reliable interconnection with a low failure probability needs to be ensured.

2 STATE OF THE ART

For module integration of BC-BJ solar cells a number of approaches exist:

- Edge interconnection (SunPower [2])
- Multi-Layer metallization (ISC [3,4])
- Interrupted fingers & wires (ISE [5])

Sketches of the three interconnection approaches are shown in Figure 1, naturally, each of the concepts features advantages and disadvantages. The edge interconnection is industrially proven and in production since 2007 [6]; the company SunPower continuously shows excellent results and highest module efficiencies. Nevertheless, this concept comes along with some drawbacks like electrical shading below the external contacts [7], long current paths in the fingers, high metal consumption, as well as a costly and demanding process sequence.

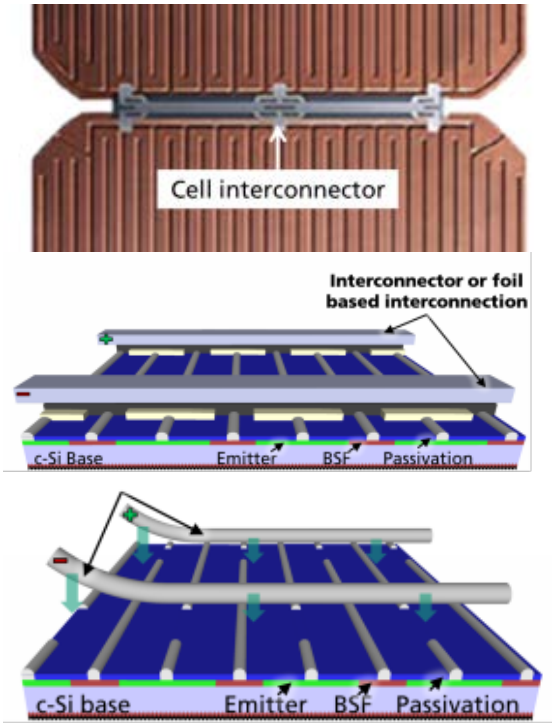

Figure 1: Top: Edge interconnection concept of BC-BJ solar cells as industrialized and used by SunPower. SunPower Maxeon®.
Middle: Multi-Layer inter-connection with continuous fingers, insulation layer und screen-printed busbars [5].
Bottom: Wire interconnection on interrupted fingers [5].

The multi-layer metallization (also known as "3D busbars") allows for narrow fingers and thereby low recombination losses and very limited electrical shading as the external contacts are separated from the silicon-metal-contact. The process sequence demands at least

three steps:

a) finger metallization for contacting BSF and emitter,
b) screen printing of an insulation layer,
c) screen printing of busbars.

These process steps result in additional expenses and material costs. A third option was published by Hendrichs *et al.* [5] interrupting every second finger and consequently interconnecting all p (respectively n) fingers with one wire. In their work, the wire interconnection is based on straight wires and requires an additional screen printing step for solder pads, providing a large enough area for reliable module interconnection [5]. Furthermore the failure probability of single pads of this interconnection concept has not been studied.

Especially the interrupted fingers & wire approach is well suited for bifacial module concepts as only a small fraction of the cell rear side is shaded by cell metallization and interconnecting wires.

3 SIMULATION AND EXPERIMENTS

We started our investigation by surveying previous results and conducting a simulation study, which was already published in 2018 by Huyeng *et al.* [8]). Based on this, we carry out a geometry variation of the solder pads and evaluate the performance of the geometries by peel tests. Furthermore, we develop the H-shaped electrode, which features a number of advantages.

3.1 Simulation

We used numerical simulation by Quokka3 [9], to simulate a BC-BJ solar cell portion, which includes 7x7 electrodes, resulting in a total simulated cell area of 45.5 mm x 10.5 mm (details given by Huyeng *et al.* [8]). This large size simulation enables us to differentiate between: a) disconnected pads which are far apart and therefore do not influence each other; b) disconnected pads along one doping area (horizontal) and c) along one interconnector wire (vertical). All of these cases are investigated for both doping areas (BSF and emitter). The neighboring pad failures are indicated in Figure 4.

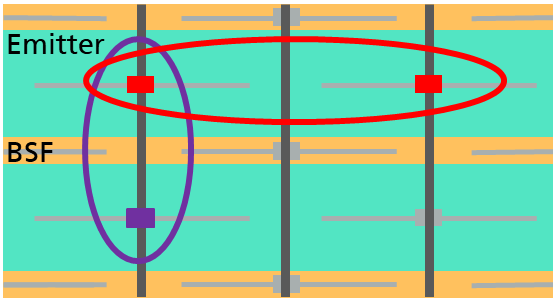

Figure 2: Sketch of a part of the simulated cell rear side. Shown are BSF and emitter areas, the metallization and possible interconnection failures. The red ellipse indicates two neighbouring pads on neighbouring wires which are disconnected. The purple ellipse indicates two disconnected pads on the same wire.

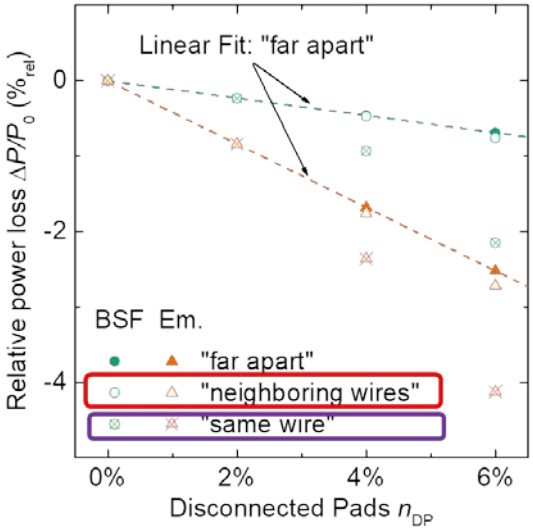

Figure 3: Results of a Quokka3 simulation of a cell fracture with 7x7 electrodes (45.5 mm x 10.5 mm). The green symbols show the relative power loss caused by disconnected BSF pads. The orange symbols indicate the relative power loss caused by disconnected emitter pads [8].

The simulation results are shown in Figure 5. The graph visualizes the relative power loss caused by a varied proportion of disconnected pads (either BSF or emitter). A linear fit is applied for the disconnected BSF and emitter pads, which are far apart. As the linear fit indicates these disconnected pads do not influence each other and therefore follow a superposition principle. As can be determined from Figure 5 the relative power losses caused by disconnected pads along the same wire are significantly higher than the losses caused by disconnected neighboring pads along one doping area. This is therefore the most significant failure mechanism and should be minimized first.

For a rough estimation the relative power loss of the BSF and emitter pads can be added up (cf. Huyeng *et al.* 2018). Consequently 6 % disconnected pads result in up to 6 % relative power loss. For a half-cell, which is targeted in this work and which features around 600 solder pads this would correspond to only 36 solder pads. Previous experience shows, that failure rates between 5 % and10 % are common for small pads.

3.2 Linear Electrode Variation

Based on the simulation we aim at finding the minimal pad geometry still allowing a reliable solder joint and reasonable peel forces. The wire target diameter is between 0.2 mm and 0.4 mm. Because of their advantages regarding mechanical stress and bowing, wave-shaped wires are used in this investigation. Figure 6 shows a sketch of a linear electrode. Based on the results from Hendrichs [5] a pad length of 1.0 mm is taken while the pad width is varied: 0.1 / 0.2 / 0.3 / 0.4 mm.

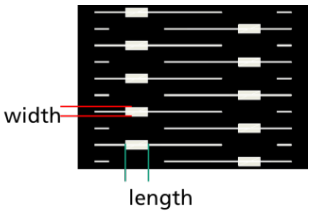

Figure 4: Sketch of linear electrodes on interrupted fingers.

The optimal pad length is a compromise between minimal finger interruption for highest efficiencies, small pad area for minimal recombination on the metal-semiconductor interface and simultaneous alignment of up to 30 wires on one cell rear side. Back contact cells inhibit the additional challenge of having to align all interconnectors on the rear side. If the soldering is conducted sunny side up, the alignment between cell metallization and interconnecting wires is not visible during the process. The shape of waved wires in general does not complicate the alignment. However, if the doping pitch and the wavelength of the wire are close to each other, the wave can lay around the pad, reducing the soldered area or even resulting in no overlap between pad and wire.

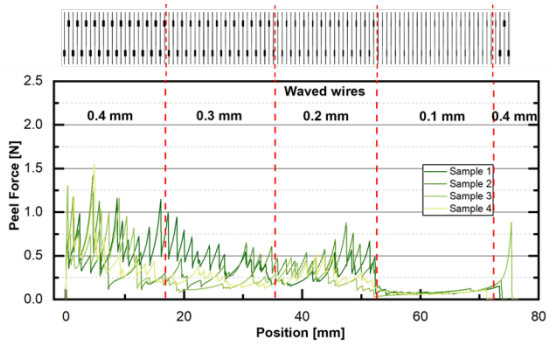

Figure 5: Force-path diagramm of peel tests using wave-shaped wires on four cell stripes with linear pads and varying pad widths between 0.1 mm and 0.1 mm. The Ag paste was printed on bare silicon.

In this study we perform all peel tests according to DIN EN 50461 [10] using wave-shaped wires with a copper core diameter of 300 µm and and a solder coating (10-15 µm) of Sn62Pb36Ag2. We preheat the samples to 120 °C on a hotplate and solder at 270 °C using a no-clean flux. Whenever peel results are shown, all samples presented in one graph were fabricated simultaneously. For standard busbar interconnection peel forces are usually normalized to the ribbon width. However, as the wetted area after soldering seems to vary between pads, we choose not to normalize these values to the pad area (0.2 mm²) or the wire/pad overlap area (0.06 mm²).

Figure 7 shows the results of peel tests of four different samples. Each force peak represents one solder pad. The measured peel forces for the pad widths between 0.4 mm and 0.2 mm are on a very good level considering the small soldering area. For a pad width of 0.2 mm all peaks are above 0.5 N. For a pad width of 0.1 mm the peel force decreases below 0.25 N, indicating that 0.2 mm is the smallest reliable pad width using the chosen Ag paste.

Based on the results of the peel tests new cell stripes are fabricated featuring only the pad geometry of 1.0 mm x 0.2 mm. These cell stripes also feature a 100 nm SiN_X capping layer on the rear side. All poorly or not connected pads (dark areas) in each taken EL image are counted and the failure rate calculated. The resulting failure rate for the linear pads is approximately 12.5 %. Three main failure reasons for the chosen pad geometry exist: a) misalignment of the wave-shaped wire, one wave may lie around the pad instead of on top of the pad; b) no solder connection is formed between wire and pad; c) rupture of the contact pad caused by low adhesion forces. Dark areas can indicate either of the failure reasons.

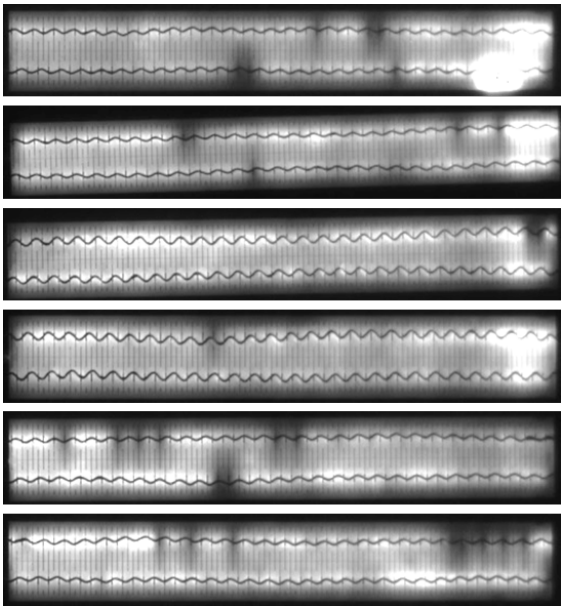

Figure 6: Electroluminescence (EL) images taken after soldering of the cell stripes with linear pads using wave-shaped wires. The pad geometry for all stripes is 1 mm x 0.2 mm. The Ag paste was printed on 100 nm SiNx.

3.3 Improved Electrode Design

Even though the linear pads show promising peel forces, the EL images show that a more reliable module interconnection is necessary. Based on the two main failure reasons for the linear pads, we introduce an improved electrode design: the H-shape (Figure 9). The H-shape simplifies the alignment between wires and soldering pads as even if the wave-shaped wire lays around two neighboring solder pads, the “H-line” still enables a reliable soldering area. The “H-line” also provides an electric redundancy between two neighboring fingers, which reduces the relative power loss if one pad is disconnected (*cf.* Sec. 3.1)

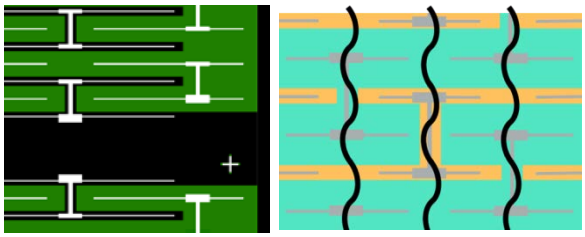

Figure 7: Left: Sketch of the central area of a wafer with two half-cells and H-shaped pads on emitter (green) and BSF (black).
Right: Sketch of H-shaped pads including interconnecting wave-shaped wires.

Implementing the H-shape only increases the total metallization fraction of one solar cell from 2.6 % for linear pads (1.0 mm x 0.2 mm) to 2.7 % for H-shaped pads, assuming a finger width of 40 µm and 52 n- and p-fingers per half-cell. The H-shape requires a change in the doping areas, as a cell approach with fire-through

paste is aimed at to prevent shunting (cf. Fig. 9). The cell efficiencies of both pad geometries are simulated and shown in Table 1.

Table 1: Simulated BC-BJ cell results. Input parameters are as in the presented 7x7 electrode simulation *cf. sec. 3.1*.

Pad shape	V_{OC} (mV)	J_{SC} (mA/cm^2)	FF (%)	η (%)
Linar	672.0	40.5	81.5	22.2
H-shape	671.9	40.5	80.8	22.0

An experiment comparing the peel forces of linear and H-shaped pads is conducted. Both geometries are applied on cell stripes with 100 nm SiN_X on a none-textured surface. The peak peal forces show t We apply a peak detection algorithm on the resulting force-path diagrams and calculate the mean value of the detected force maxima. The results are shown in Figure 10. The very low peel forces of the linear pads compared to the forces shown in Figure 7 are most likely caused by the introduced capping layer of 100 nm SiN_X. In this study only one Ag paste was tested, other Ag pastes can result in higher peel forces [12]. Nevertheless, the investigation shows a significant advantage for H-shaped pads, which is higher than the proportional advantage of the larger pad area (1:1.65), indicating that the geometry itself is of advantage for this interconnection approach. Based on these results the H-shaped pad geometry with a width of 0.2 mm was applied on BC-BJ solar cells.

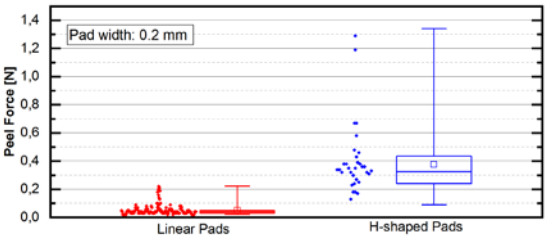

Figure 8: The graph shows the peel forces of linear and H-shaped pads with a width of 0.2 mm using wave-shaped wires.

3.4 Application on BC-BJ solar cells

As the H-shaped electrode geometry shows significant advantages on cell stripes we apply the structure on BC-BJ half-cells with according doping layout, passivation on the rear side and a 100 nm SiN_X capping layer. The fabricated half-cells are interconnected for later module integration. Peel tests are conducted on a number of half-cells. The results of three half-cells on which six peel tests are conducted on p- as well as on n-type pads are summarized in Figure 11. With respect to the pad area and thereby possible soldering area all six rows show sufficient peel forces for module integration. The rather large differences between the six rows might be caused due to the lab setup used for the soldering process. Nevertheless all wires were aligned precise enough to enable a reliable soldering process.

Electroluminescence (EL) images of soldered half cells are taken. One representative EL image is shown in Figure 12. The image displays a quite homogeneous interconnection of 564 out of the 600 pads. Some areas look poorly, very few not connected. A statistical analysis of all EL images shows that a failure rate of approximately 4.5 % occurs for the presented parameters.

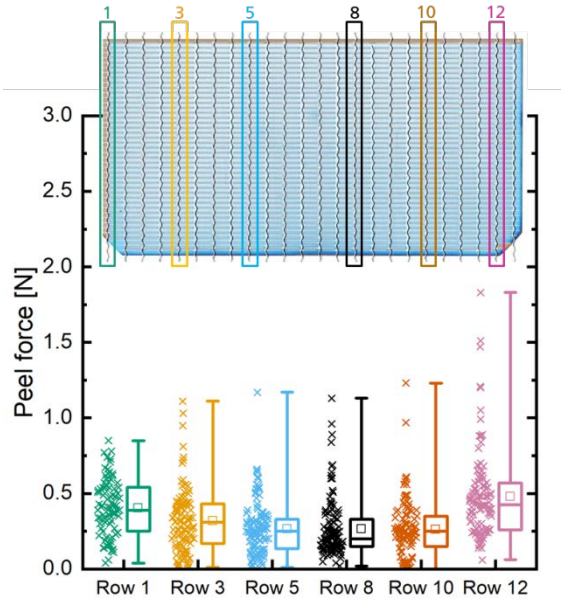

Figure 9: The graph shows the forces measured during a peel test of H-shaped pads with a width of 0.2 mm.

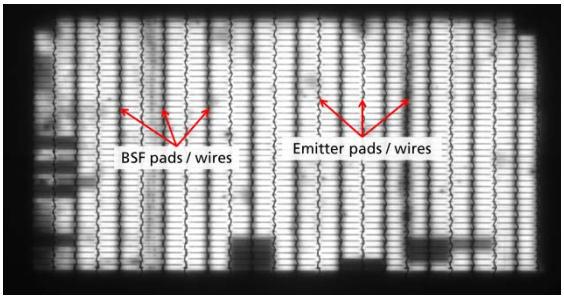

Figure 10: Electroluminescence image of a representative BC-BJ half-cell with 300 H-shaped pads (0.2 mm wide) and interconnected with 24 wave-shaped wires.

4 CONCLUSIONS

Our investigation shows that based on peel test results the minimal pad width of linear soldering pads for BC-BJ solar cells can be reduced down to 0.2 mm. The presented simulation shows that the detected failure rate of the linear pads of 12.5 % would lead to a significant power loss. Assuming equal distribution between BSF and emitter pads the power loss can be over 12 % relative.

The introduced H-shape electrode geometry shows two significant improvements:

- Increase of mean peel force from below 0.1 N for linear pads to above 0.3 N for H-shaped pads with the used metallization paste.
- Decrease of failure rate from 12.5 % for linear pads down to 4.5 %.

The possibility of further improving the failure rate will be investigated and if successful be presented in a following publication. H-shaped pads with wave-shaped wires can contribute to further reduce the costs of BC-BJ module fabrication while ensuring reliable

interconnection.

Furthermore the presented interconnection approach is perfectly suitable for bifacial concepts as only 2.7 % of the cell rear side is metallized. In combination with wire interconnection this should result in a very high bifaciality.

5 ACKNOWLEDGEMENTS

This work was supported by the German Federal Ministry for Economic Affairs and Energy within the research project “Backbone” under contract number 0324057B. The authors thank our project partners from Schmid for the fruitful discussions and all coworkers at Fraunhofer ISE’s PV-TEC for assistance with sample processing, characterization and discussion.

5 REFERENCES

[1] L. C. Rendler et al., “*Wave-shaped wires soldered on the finger grid of solar cells: Solder joint stability under thermal cycling*” in SiliconPV *2018*, p. 80001.

[2] SunPower website, c. 2019, [accessed 2019 Sept. 8] https://www.sunpower.de/produkte/maxeon-solarmodule

[3] G. Galbiati et al., “*Large-area back-contact back-junction solar cell with efficiency exceeding 21%*”, Proc. 38th IEEE PVSC, Austin, TX, 2012

[4] S. DeVecchi et al., “*New Metallization Scheme for Interdigitated back Contact Silicon Heterojunction Solar Cells*” Energy Procedia, Vol. 38, 2013, Pages 701-706

[5] M. Hendrichs et al., „*Screen-Printed Metallization Concepts for Large-Area Back-Contact Back-Junction Silicon Solar Cells*”, IEEE JPV, VOL. 6, NO. 1, 2016

[6] SunPower website, c. 2019, [accessed 2019 Sept. 8] https://us.sunpower.com/company/history,

[7] M. Hermle et al., “*Shading Effects in Back-Junction Back-Contacted Silicon Solar Cells*”, Proc. 33rd IEEE PVSC, St. Diego, CA, 2008

[8] Huyeng et al., “*Towards all screen printed back-contact back-junction silicon solar cells*”, Proc. 8th SiliconPV, Lausanne, CH, 2018

[9] A. Fell, et al., “*The concept of skins for silicon solar cell modeling*”, Sol. Energy Mater. Sol. Cells 173, p. 128-133, 2017

[10] *Solarzellen - Datenblattangaben und Angaben zum Produkt für kristalline Silicium-Solarzellen*, EN 50461: 2007-03, 2007.

[11] J. Walter et al., “*Multi-wire Interconnection of Busbar-free Solar Cells*”, *Energy Procedia*, vol. 55, pp. 380–388, 2014.

[12] J.D. Huyeng, et al., “*Simultaneous Contacting of Boron and Phosphorus Doped Surfaces with a Single Screen Printing Paste*”, *this conference*